ARCTIC
VOL. 42, NO. 3 (SEPTEMBER 1989) P. 253-264

A Benign, Small-Scale Power Unit for the Arctic: The Carnot Cycle Concept

G.S.H. LOCK[1]

(Received 8 February 1988; accepted in revised form 8 February 1989)

ABSTRACT. Small amounts of useful power may be generated in polar or subpolar regions during the winter period by placing a heat engine between a large body of water (near 0°C), acting as a heat source, and the atmosphere (near −25°C), acting as a heat sink. The scheme consists of a fuelless modular system operating on the Carnot cycle. Power is extracted by a reciprocating vapour engine drawing saturated vapour from a water-heated evaporator and exhausting to an air-cooled condenser from which nearly saturated liquid is returned to the evaporator using a reciprocating feed pump.

The thermal performance model incorporates both the engine cycle power and the parasitic losses, the latter being incurred as a result of circulating the working fluid (ammonia), pumping water through the evaporator and blowing air through the condenser. Curves indicate power levels in excess of 1 kW, with thermal efficiencies around 5%. The power curves show a maximum with respect to speed.

The principal difficulties with this scheme are in heat exchanger design in near-freezing water. The principal advantages are small power levels, flexibility through modular construction and reduction of the capital and operating costs associated with the supply of energy to northern regions.

Key words: alternative energy, Carnot, OTEC, heat engine, power

RÉSUMÉ. De petites quantités d'énergie utile peuvent être produites dans les régions polaires ou subpolaires au cours de la période hivernale, en plaçant une machine thermique entre une importante masse d'eau (près de 0°C), agissant comme une source de chaleur, et l'atmosphère (près de −25°C), agissant comme un puits de chaleur. L'appareil fait appel à un système modulaire sans carburant fonctionnant sur le cycle de Carnot. L'énergie est extraite par une machine à vapeur à mouvement alternatif qui tire de la vapeur saturée d'un évaporateur chauffé à l'eau et la laisse s'échapper dans un condenseur refroidi par l'air, duquel le liquide presque saturé est renvoyé à l'évaporateur grâce à une pompe d'alimentation à mouvement alternatif.

Le modèle de performance thermique intègre à la fois l'énergie du cycle de la machine et les pertes parasites, celles-ci étant dues au fait qu'on doit faire circuler le fluide de travail (de l'ammoniac), pomper de l'eau dans l'évaporateur et souffler de l'air dans le condenseur. Les courbes indiquent des niveaux de puissance supérieurs à 1 kW, avec des efficacités thermiques d'environ 5%. Les courbes de puissance en fonction de la vitesse montrent un maximum.

Les principales difficultés avec ce système concernent la conception de l'échangeur de chaleur dans de l'eau proche du point de congélation. Les principaux avantages sont les faibles niveaux de puissance, la souplesse due à la construction modulaire et la diminution des coûts en capital et des coûts d'exploitation reliés à la demande d'énergie dans les régions nordiques.

Mots clés: énergie alternative, Carnot, conversion de l'énergie thermique de l'océan, machine thermique, force motrice

Traduit pour le journal par Nésida Loyer.

INTRODUCTION

> Everyone knows that heat can produce motion. That it possesses vast motive-power no one can doubt, in these days when the steam-engine is everywhere so well known.
>
> To heat also are due the vast movements which take place on the earth. It causes the agitations of the atmosphere, the ascension of clouds, the fall of rain and of meteors, the currents of water which channel the surface of the globe, and of which man has thus far employed but a small portion. Even earthquakes and volcanic eruptions are the result of heat.
>
> From this immense reservoir we may draw the moving force necessary for our purposes. Nature, in providing us with combustibles on all sides, has given us the power to produce, at all times and in all places, heat and the impelling power which is the result of it. To develop this power, to appropriate it to our uses, is the object of heat-engines.
>
> The study of these engines is of the greatest interest, their importance is enormous, their use is continually increasing, and they seem destined to produce a great revolution in the civilized world.

These are the opening lines of Carnot's "Reflections on the motive power of fire, and on machines fitted to develop that power" written in 1824 (Carnot, 1960:16). They are not only prophetic, anticipating the enormous impact of the heat engine all over the world, but curiously romantic, especially for a military engineer. Nature is seen as the source of mankind's benefits, and the heat engine in particular is seen as a very natural development. This view of technology is not prevalent today.

The human demand for energy has increased considerably since Carnot first wrote the above words and has risen dramatically during the past few decades. Conventional uses of energy have become more widespread and new uses continue to appear. Despite fluctuations from year to year, the general demand shows no sign of abating, a fact accompanied by increases in the costs and prices of non-renewable energy. At the same time, the products of many energy-absorbing processes are found to be injurious to health.

The search for alternative energy sources has been in progress for some time and now a wide range of limited, but benign, forms is currently under consideration. Among these are geothermal and hydrothermal energy, for which the sources are respectively the earth and large bodies of water. The second of these, which is our main interest here, has received widespread attention in the context of ocean thermal energy conversion (OTEC); this is applicable in climates where the surface layers of the ocean are much warmer than the water found at depth. A heat engine operating between these two temperature levels, which are roughly 20 K apart (Taylor, 1983), is capable of producing power with a Carnot efficiency approaching 8%, at least in principle.

Typically, the OTEC concept is viewed in terms of a stationary plant generating large powers (e.g., 100 MW) using turbomachinery operating on a Rankine cycle. Representative

[1]Department of Mechanical Engineering, University of Alberta, 4-9 Mechanical Engineering Building, Edmonton, Alberta, Canada T6G 2G8

NOMENCLATURE

A	surface area (m^2)
c_p	specific heat ($J \cdot kg^{-1}K^{-1}$)
c_r	clearance ratio
d	tube diameter (m)
f	parasitic power (W), friction factor
F	fouling factor, boiling factor
G	mass flow velocity ($kg \cdot m^{-2}s^{-1}$)
h	heat transfer coefficient ($W \cdot m^{-2}K^{-1}$)
k	thermal conductivity ($W \cdot m^{-1}K^{-1}$)
m	mass (kg)
n	index of expansion, compression
N	rotational speed (rps)
P	absolute pressure (Pa)
Pr	Prandtl number
q	heat flux density ($J \cdot m^{-2}s^{-1}$)
Q	heat transfer (J)
R	gas constant ($J \cdot kg^{-1}K^{-1}$)
r_c	cutoff ratio
r_p	pressure ratio
Re	Reynolds number
S	suppression factor
t	thickness
T	absolute temperature (K)
U	overall heat transfer coefficient ($W \cdot m^{-2}K^{-1}$), velocity ($m \cdot s^{-1}$)
v	specific volume ($m^3 \cdot kg^{-1}$)
V	volume (m^3)
w	specific work ($J \cdot kg^{-1}$)
W	work (J)
x	mixture quality
Z	correction factor

Greek Letters

γ	ratio of specific heats
Δ	increment
η	efficiency
θ	temperature loss (K)
λ	latent heat ($J \cdot kg^{-1}$)
ρ	density ($kg \cdot m^{-3}$)
τ	torque (Nm)

Superscripts

·	per unit time
C	condenser
E	evaporator

Subscripts

a	air
c	condenser, cycle, convection
CAR	Carnot
e	expander
E	evaporator
f	feed pump
FAN	fan
i	ice, inside, induced
is	isentropic
l	liquid
m	mixture
NB	nucleate boiling
o	outside, overall
opt	optimum
OFF	offtake
PUM	water pump
R	ratio
s	shaft
SAT	saturated
TH	thermal
v	vapour, per unit volume
w	wall

OTEC studies have wisely concentrated on heat exchanger development (Uehara *et al.*, 1984; Mochida *et al.*, 1984). Efficiency figures are not widely quoted, partly because the pumping power required to lift the cooler water to the surface is rather uncertain. This power must be subtracted from the gross engine power, thus reducing both the useful power output and the efficiency. It is estimated that achievable thermal efficiencies would be of the order of 2% (Taylor, 1983; El-Wakil, 1984).

Hydrothermal energy in a northern context, in which the heat source is a body of water and the heat sink is the winter wind, has received less attention, despite the fact that temperature differences and theoretical thermal efficiencies are likely to be greater. Figure 1 uses the freezing index as a measure indicating the viability of the scheme: the contour 4500, for example, corresponds to an air temperature of −25°C maintained for about three months. It is thus clear that huge areas of Alaska, northern Canada, Greenland and the U.S.S.R. exhibit suitable temperature-time characteristics. Thus far, studies appear to have followed the OTEC pattern (Swartman and Green, 1978; Haydock, 1985). In particular, the report prepared for the Canadian Electrical Association by Acres Ltd. presents a detailed analysis of a large-scale steady flow system capable of generating power levels of the order of 2 MW. Two features become apparent: thermal efficiencies are likely to be at least as high as those attainable in tropical OTEC systems, and economic power levels may be too great for all but a few large communities near the arctic circle.

The concept advanced in this paper attempts to incorporate the higher theoretical efficiencies attainable in the polar and sub-polar environment, while circumventing the disadvantages of large-scale, high-speed machinery. To this end, attention will be focussed on the analysis and design of a 1 kW engine running at speeds low enough to render internal frictional losses negligible. Assessment will be based on the most efficient thermodynamic cycle known: namely, the Carnot cycle. The successful design of such a power module will permit the highest possible thermal efficiencies to be maintained, virtually independent of engine size. The device will therefore be applicable in a wide range of circumstances, including those appropriate to small communities and remote scientific stations. Equally important, it may achieve Carnot's romantic ideal of a benign heat engine working in harmony with nature to benefit human society without inflaming demand or polluting the environment.

THERMODYNAMIC THEORY

The Carnot cycle, perhaps the best known of all thermodynamic cycles, consists of four ideal processes: isentropic expansion, isothermal cooling, isentropic compression and

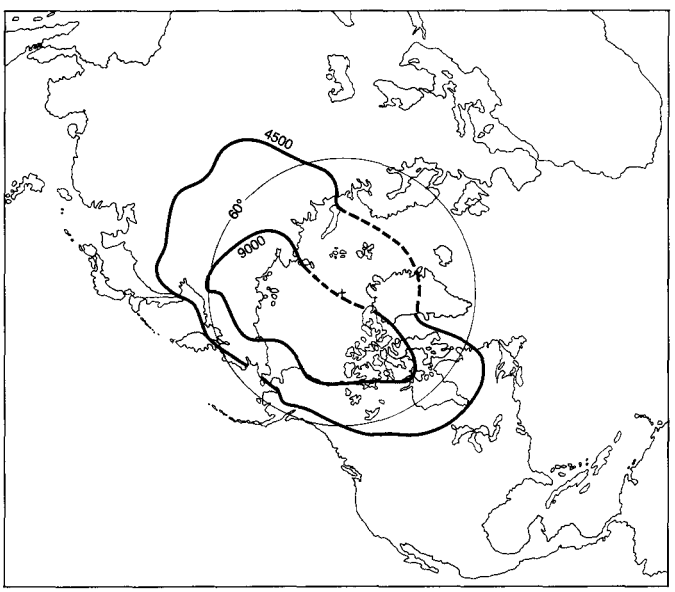

FIG. 1. Freezing indices in the northern hemisphere.

isothermal heating. If these processes are carried out entirely within the liquid-vapour region, the system may be represented by the schematic shown in Figure 2. Warm water taken from beneath a winter ice cover will have a temperature close to the equilibrium freezing value T_i: this is the source used to convert saturated liquid at T_1 and P_1 to dry saturated vapour at $T_2=T_1$ and $P_2=P_1$. Cold winter air at temperature T_a causes high-quality vapour at T_3 and P_3 to condense, thereby producing low-quality vapour at $T_4=T_3$ and $P_4=P_3$. Between the saturation pressures P_2 and P_3 a reciprocating expander extracts useful work while a reciprocating feed pump operating between the same pressures subtracts work.

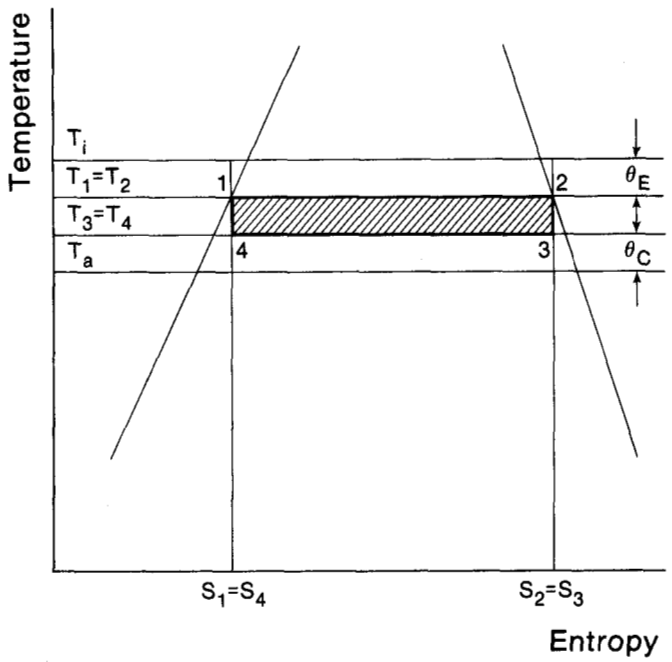

FIG. 2. Carnot cycle in relation to ambient temperature.

Under ideal conditions the cycle produces a net specific work of

$$w_c = w_e - w_f \quad (1)$$

with a thermal efficiency of

$$\eta_{TH} = \frac{w_c}{q_E} = \frac{w_c}{\lambda_{12}} = 1 - \frac{T_4}{T_1} \quad (2)$$

from which it follows that

$$w_c = \lambda_{12}\left(1 - \frac{T_4}{T_1}\right) \quad (3)$$

It is thus clear that for given temperature limits the ideal net work is determined directly by the latent heat of evaporation at the upper saturation pressure.

Table 1 compares a selected list of suitable working fluids (Rzanjevic, 1976; ASHRAE, 1985). The potential list is very long but these four are representative. From a thermodynamic point of view, ammonia is clearly the superior fluid. It is also attractive from a mechanical standpoint because the saturation pressures near the representative environmental temperatures of $T_i=0°C$ and $T_a=-25°C$ are not great enough to require high-pressure design standards, but they are greater than atmospheric and therefore eliminate the possibility of air leaking into the system.

TABLE 1. Properties of suitable fluids

Fluid	T_{CR} (K)	P_{CR} (MPa)	Saturation Pressures 273°K (MPa)	248°K (MPa)	Latent heat ($kJ \cdot kg^{-1}$)
Freon 12	385	4.113	0.309	0.124	155.9
Methyl chloride	416.1	6.674	0.256	0.107	405.1
N butane	425.0	3.794	0.101	0.036	410.0
Ammonia	406.0	11.417	0.429	0.151	1262.4

A review of relevant health implications (Gosney, 1982) reveals that ammonia is probably the least desirable of those listed in Table 1. Freon 12 and n-butane, for example, are evidently not toxic, whereas ammonia has low-threshold limit values: 25 ppm for the time-weighted average and 35 ppm for the short time-exposure limit. It is thus clear that caution must be exercised. To this end, it is explicitly understood that the system must never be used in any enclosed working or living space. Given that proviso, the use of ammonia should not create a health hazard. The total charge of the system is anticipated to be of the order 1 kg or less. Consequently, if accidental leakage does occur, the charge would be rapidly dissipated in the environment, and thus be rendered harmless. Alternatively, the entire system could be encased in a sealed space with an ammonia detector installed internally. If neither of these alternatives is acceptable, a more benign fluid would have to be used and a lower power output tolerated.

Under real conditions, the specific power indicated in equations (1) and (3) would be modified. In particular, the expander work output would be reduced. The equality of the heat and work differences given in equation (1) applies to ideal (isentropic) work processes and would therefore not apply to the actual work terms given by

$$w_{se} - w_e\eta_{is} \text{ and } w_{sf} - w_f/\eta_{is} \quad (4)$$

where η_{is} is the isentropic efficiency of the equivalent processes executed between the same pressure limits. The actual cycle power is thus given

$$\dot{W}_c = (w_{se} - w_{sf})\dot{m}$$
$$= (w_{se} - w_{sf})m_iN$$

or $$\dot{W}_c = \tau N \quad (5)$$

where $\tau = (w_{se} - w_{sf})m_i$ is the torque generated through the cycle work.

The useful power delivered is less than the cycle power by virtue of losses, which take two principal forms: the frictional power $\dot{W}_F$ required to circulate the working fluid and overcome rubbing forces between components; and the frictional power dissipated by the auxiliaries in the evaporator and condenser. The second of these, which is by far the larger, is supplied to the water pump and air fan and has been designated as auxiliary or offtake power $\dot{W}_{OFF}$. The net useful shaft power delivered by the system is thus given by

$$\dot{W}_s = \dot{W}_c - \dot{W}_F - \dot{W}_{OFF} \quad (6)$$

in which

$$\dot{W}_{OFF} = \dot{W}_{FAN} + \dot{W}_{PUM}$$

both of which, like $\dot{W}_F$, are assumed to be functions of engine speed; thus

$$\dot{W}_F + \dot{W}_{FAN} + \dot{W}_{PUM} = f(N)$$

The useful shaft power given by equation (6) may therefore be written

$$\dot{W}_S = \tau N - f(N) \quad (7)$$

This is a simple and convenient result, which will be explored more fully in later sections.

The efficiency of the system may be estimated in a number of ways. In relation to the cycle-operating temperatures, an ideal (Carnot) efficiency was given earlier by equation (2). In relation to the environmental temperatures, the most appropriate measure would again be a Carnot efficiency given by

$$\eta_{CAR} = 1 - \frac{T_a}{T_i} \tag{8}$$

The overall efficiency of the actual system is perhaps best defined by

$$\eta_o = \frac{w_s}{\lambda_{12}} \tag{9}$$

where $w_s = \dot{W}_s/\dot{m}$. The extent to which η_o approaches the maximum permissible efficiency is given by the efficiency ratio

$$\eta_R = \eta_o/\eta_{CAR} \tag{10}$$

These measures of efficiency will be used in assessing the system design below.

THE MACHINERY

As indicated earlier, it is proposed that the expander be a reciprocating device that, for greater compactness and smoothness of running, will be a double-acting type. Poppet valves are preferred over slide valves. The machine cycle for this device, represented in the pressure-volume domain, is shown in Figure 3. A typical pressure ratio is envisaged in the range $2 < r_p < 2.5$, which suggests that single expansion is adequate: multiple expansion offers little benefit for pressure ratios less than about 8:1 (McNaughton, 1948). Admission of dry saturated vapour from *a* to *b* ends in cutoff when the inlet valve is closed. From *b* to *c* expansion takes place, ideally under adiabatic conditions: it ends abruptly with the opening of the exhaust valve and a sudden release of pressure from *c* to *d*. The exhaust process follows from *d* to *e*, and the cycle is completed when the exhaust valve has been closed at *e* and rapid compression from *e* to *a* restores the volume of enclosed vapour to V_a.

Defining the cutoff ratio by

$$r_c = (V_b - V_a)/(V_c - V_a)$$

and clearance ratio by

$$C_r = V_a/(V_c - V_a)$$

the indicated specific work produced in this theoretical machine cycle may be expressed as

$$w_c = \frac{v_2 P_3(1+C_r)}{r_c(1-n)}\left[r_p\left(\frac{C_r+r_c}{1+C_r}\right)^n - nr_p\left(\frac{r_c}{1+C_r}\right) - n\left(\frac{C_r r_p^{1/n}}{1+C_r}-1\right) - 1\right] \tag{11}$$

This may be optimized with respect to the cutoff ratio for any pair of pressure and clearance ratios. Figure 4 shows typical curves (with $C_r = 5\%$) and reveals that the optimum cutoff ratio for this sytem is in the range $40\% < r_c < 60\%$.

A more precise interpretation is found in Figure 5, which shows the optimum cutoff ratio plotted over the anticipated pressure range for two different expansion indices. (Expansion and compression are assumed to follow the same polytropic law $Pv^n = C$.) The higher value of $n = \gamma$ corresponds to ideal (reversible) conditions when the process is isentropic. The lower value also corresponds to ideal conditions but the adiabatic constraint has been relaxed in order to accommodate the empirical fact that saturated vapour does not behave like superheated vapour. For saturated water vapour, the ratio of n/γ is about 0.873 (Rogers and Mayhew, 1967). Assuming the same ratio for ammonia, $n = 1.13$. It is evident from Figure 5 that the expansion index does not radically alter the optimum cutoff ratio.

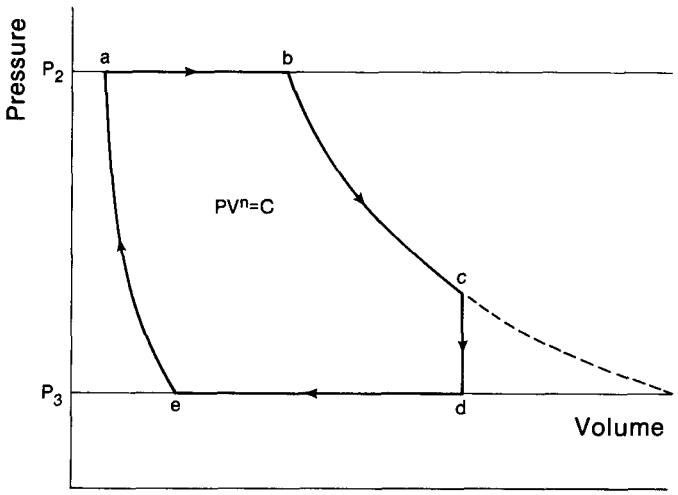

FIG. 3. Machine cycle of expander.

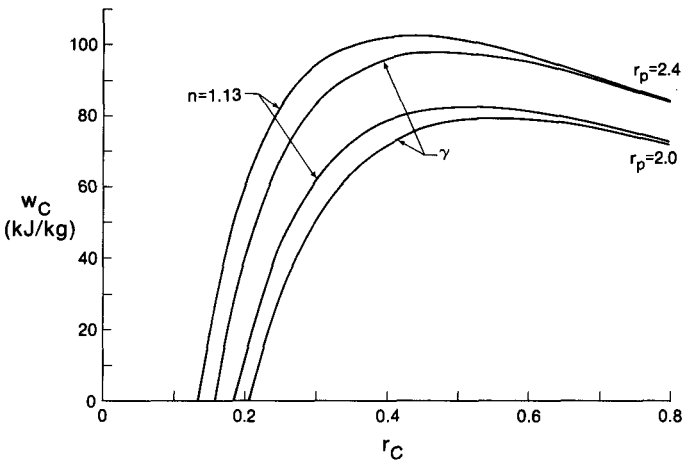

FIG. 4. Effect of cutoff ratio on specific cycle work.

In practice, the ammonia vapour is unlikely to be either superheated or supercooled, and therefore the lower index would appear to offer the better approximation. Using this index, the cycle work expressed as a fraction of the isentropic enthalpy change between the same saturation pressure limits has been plotted against the cutoff ratio (Fig. 6) for several values of temperature loss θ (which correspond to certain pressure ratios). In essence, these are curves of isentropic efficiency under ideal (reversible, non-adiabatic) conditions and reveal very high values over the range of interest. To accommodate dissipative effects, this efficiency must be multiplied by another factor less than 1.0; arbitrarily, this dissipative factor has been chosen as 0.90 to reflect the fact of slow speed operation. It is thus evident that the effective overall isentropic efficiency of the reciprocating expander is about 90%.

In the absence of any information to the contrary, the isentropic efficiency of the feed pump has been taken equal to that of the expander. This choice is one of convenience but is defensible on the grounds that the work required to drive

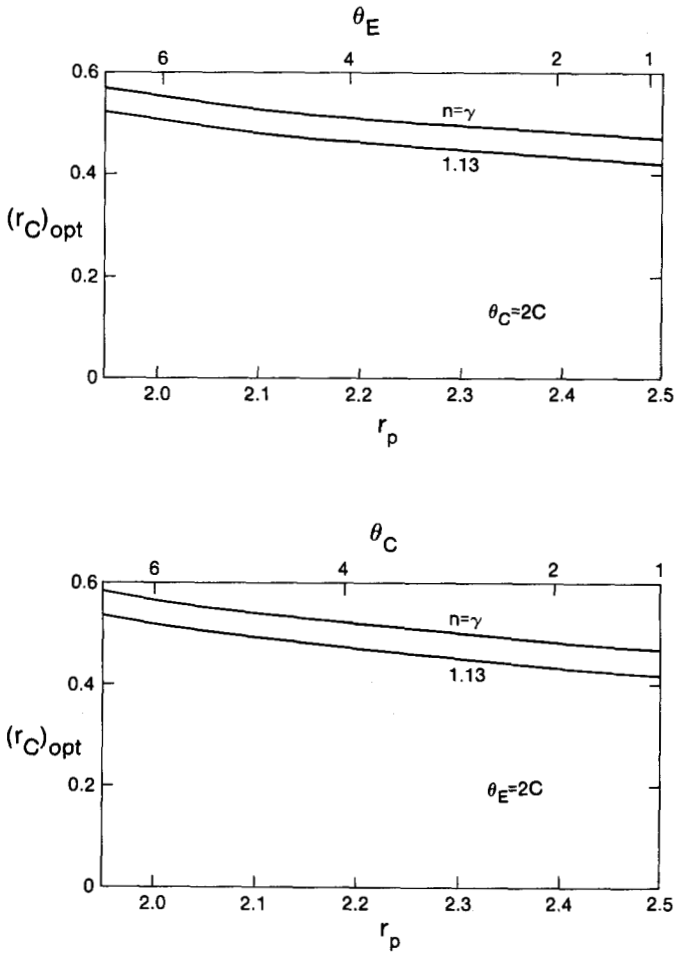

FIG. 5. Variations in optimum cutoff ratio.

the feed pump is very much less than that delivered by the expander. The power required for the feed pump could, in principle, be supplied through direct coupling with the expander piston or connecting rod. In practice, however, the same effect may be produced through the more flexible arrangement of connecting both to a common crankshaft. As discussed more fully later, the use of phase opposition leads to a smoother torque-crank angle curve.

As the T-S diagram reveals, the feed pump, unlike the expander, must be able to handle vapour of very low quality. An initial examination of the centrifugal type of feed pump (Warring, 1984) revealed that vapour tends to collect in the eye of the impeller, thus impeding entrance of the liquid. This difficulty does not occur with a reciprocating type. For compactness, double action has again been selected along with spring-loaded poppet valves. The proposed design is thus very similar to that of a conventional water feed pump, the principal differences lying in the properties of the fluid and the presence of a small amount of vapour.

If both the liquid and vapour were incompressible, the cycle-specific work for the feed pump would be given simply by

$$w_f = v_\ell(P_1 - P_4) \qquad (12)$$

But the vapour is highly compressible, and hence the mixture follows a pressure-volume relation in which the mixture specific volume is given by

$$v_m = xv_v + (1-x)v_\ell$$

Assuming the vapour obeys the ideal gas law, that its specific volume is much greater than that of the liquid, and that the mixture quality is a linear function of pressure between P_4 and P_1, a correction to equation (12) may be found. This is given by

$$\Delta w_f = -x_4\, RT \left[1 - \frac{P_1}{(P_1 - P_4)} \ln \frac{P_1}{P_4}\right]$$

However, this reduction represents only a small fraction of w_f, which in turn is only a small fraction of w_e, and therefore equation (12) has been used in the calculations presented below.

THE HEAT EXCHANGERS AND AUXILIARIES

For a Carnot cycle efficiency of the order of 10%, heat transfer rates in both the evaporator and condenser are much greater than the difference between them, the net theoretical power output. To obtain a useful power output of 1.0 kW, it was estimated initially that the gross power level may have to be 50% greater than this value in the selected design speed range of 60-120 rpm. Accordingly, heat transfer rates in the evaporator and condenser were each set at the nominal value of 15 kW. In both devices the heat transfer rate is given by

$$\dot{Q} = UA\theta \qquad (13)$$

in which θ is the appropriate temperature difference during the heat transfer. In each instance, a single-pass cross flow arrangement was considered so that

$$\theta = \left(\frac{\Delta T_2 - \Delta T_1}{\ln \dfrac{\Delta T_2}{\Delta T_1}}\right)$$

where the subscripts 1 and 2 represent the opposite ends of the heat exchanger if it were to operate in the counterflow mode.

In the evaporator, the ammonia follows a forced convection boiling process akin to flash evaporation. Heat transfer coefficients are likely to be in the range 10^3-10^4 $W \cdot m^{-2}$-K. The water flow system must match the boiling heat transfer rates but, as a single-phase system, may be expected to exhibit lower heat transfer coefficients. To allow greater flexibility in the control of water heat transfer coefficients, the design is based on the assumption that the water is on the shell side of the heat exchanger while the ammonia is on the tube side.

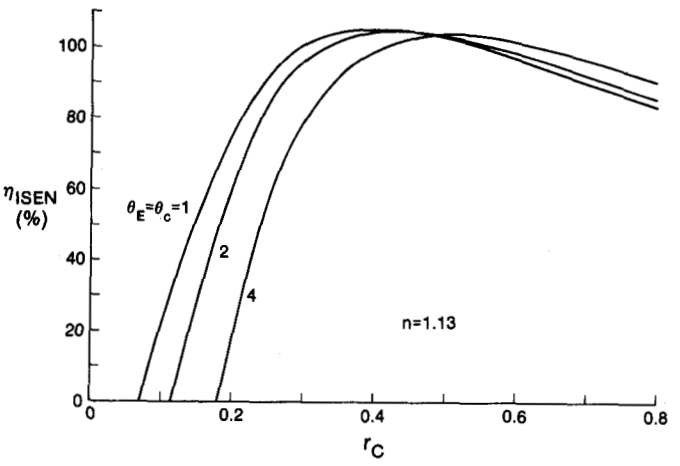

FIG. 6. Effect of cutoff ratio on isentropic efficiency.

Despite the pulsatile nature of the feed pump delivery, the evaporative process is taken to be one of forced convection boiling in which the quality changes from 0 to 1.0 over the tube length, and thus provides dry-saturated vapour for admission to the expander. Under steady conditions, the average tube side heat transfer coefficient is given by (Chen, 1966):

$$h_i^E = h_{NB} + h_c \quad (14)$$

where $h_{NB} = 0.00122 \left[\frac{k_\ell^{0.79} c_{p\ell}^{0.45} \rho_\ell^{0.49}}{\sigma^{0.5} \mu_\ell^{0.29} \gamma_{12}^{0.24} \rho_v^{0.24}} \right] (\triangle T_{SAT})^{0.24} (\triangle P_{SAT})^{0.75} S$

and $h_c = 0.023 \left(\frac{k_\ell}{d_i}\right) Re_\ell^{0.8} Pr_\ell^{0.4} F$

$\triangle T_{SAT} = T_w - T_{SAT}$ while $\triangle P_{SAT}$ is the difference in the saturation pressures at these two temperatures. For the range of conditions to be considered here, this reduces to

$$h_i^E = 1.6 (\triangle T_{SAT})^{0.24} (\triangle P_{SAT})^{0.75} + 196N^{0.8} \quad (15)$$

It is worth noting that the speed-sensitive term typically represents about 10% of the total in this expression.

On the shell inside of the evaporator, the single-phase forced convection process appropriate to cross flow over a bank of tubes may be represented by (Zukauskas, 1972)

$$Nu_d^E = CRe_d^{m1} Pr^{m2} (Pr/Pr_w)^{1/4} \quad (16)$$

For water flowing over 210 tubes of $d_i = 0.0125$ m, $d_o = 0.0171$ m and length 1.5 m spaced 3 d_o apart in 21 rows spaced 1.5 d_o apart, this expression reduces to

$$h_o^E = 33.56\, Re_d^{0.6} \quad (17)$$

The overall heat transfer coefficient may be found by substituting equations (15) and (17) into

$$\frac{1}{U_E} = \left[\frac{1}{h_i^E} + \frac{1}{h_o^E} + F_i + F_o \right] \quad (18)$$

in which fouling coefficients have been estimated (TEMA, 1959) at $F_i = 1.8 \times 10^{-4}$ m^2–K/W and $F_o = 8.8 \times 10^{-5}$ m^2–K/W, and the thermal resistance of the tube wall has been ignored. The effective temperature difference driving the evaporator heat flux simplifies to $\theta = \theta_E$ because the change in water temperature is small enough (0.1°C or less) to permit the use of the approximation

$$\ln \triangle T_2^E / \triangle T_1^E \simeq (\triangle T_2^E - \triangle T_1^E) / \triangle T_1^E.$$

The above analysis enables the evaporator heat transfer rate to be determined from the form (13) given θ_E, the surface area implicit in equation (17), and the implicit water flow rate. However, it does so by ignoring periodicity in the feed pump discharge. This pulsatile effect may be examined by first noting that the discharge takes place over 80 degrees during each stroke. Representing the mass pulse sinusoidally, the instantaneous mass flow rate may then be averaged over time, and hence over the entire stroke, by assuming that quasi-steady conditions prevail. The resulting integration reveals only a small change in h_i^E, the consequent alteration in U_E being typically a few percent, and thus justifying the quasi-steady assumption. In view of this finding, the results given below will be based on the simpler steady flow analysis.

The power required to produce these evaporator heat transfer coefficients must be tapped from the engine shaft, directly or indirectly. The pressure drop across a bank of tubes is given by (Zukauskas, 1972)

$$\triangle P = fZNG^2_{max}/2\rho \quad (19)$$

For the conditions and configurations given, this reduces to

$$\triangle P = 4.59 \rho_w U^2_{max} \quad (20)$$

implicit in which is the water flow rate. Combining the latter with equation (20), it is found that

$$\dot{W}_{PUM} = 2.35 \rho_w U^2_{max} \quad (21)$$

is the power required for water circulation within the evaporator.

The treatment of the condenser is not materially different from that of the evaporator. Again it may be assumed that heat transfer coefficients characteristic of condensation will be much greater than those anticipated for single-phase forced convection, especially when the fluid is air. In fact, it is to be expected that the lowest heat transfer coefficients in the entire system would be associated with the air flow. Accordingly, the air has been located on the shell side of the condenser in order to retain design flexibility.

Given a single-pass cross flow arrangement, the forced convective flow of air over a bank of tubes is described by equation (16). For 1500 tubes of $d_i = 0.0125$ m, $d_o = 0.0171$ m and length = 2.0 m, spaced 1.5 d_o apart in 50 rows spaced 1.5 d_o apart, it is found that

$$h_o^c = 0.46 Re_d^{0.6} \quad (22)$$

in which the coefficient is seen to be considerably lower than that appropriate to water and given in equation (17). As expected, the functional form remains the same.

Inside the tubes, the process might be described as forced periodic film condensation, about which little is known. Under steady conditions, the process may be modelled, conservatively, by the expression (Chato, 1962)

$$h_i^c = 0.55 \left[\frac{g\rho_l(\rho_l - \rho_v)k^3_l \lambda}{\mu_l (T_v - T_w) d_i} \right]^{1/4}$$

which for ammonia condensing in the given tubes reduces to

$$h_i^c = 13{,}800/(T_v - T_w)^{1/4} \quad (23)$$

This simple expression has two significant features. Firstly, the ammonia flow rate is absent, and therefore direct transient effects are absent; they do, however, enter through the effect of flow rate on T_w (which alters with a changing heat balance). It is thus expected that the effect of pulsatility is even less evident in the condenser than in the evaporator. The second feature is the magnitude of h_i^c when $T_v - T_w \ll 1$. Although values higher than 13 800 W·m^{-2}K^{-1} have been reported in the heat transfer literature, it was decided to limit h_i^c to a conservative value of 1000 W·m^{-2}K^{-1}.

The overall heat transfer coefficient was obtained by substituting equations (22) and (23) into

$$\frac{1}{U_c} = \frac{1}{h_i^c} + \frac{1}{h_o^c} + F_i$$

where F_i has been taken as 1.8×10^{-4} m^2 K·W^{-1} (TEMA, 1959).

Unlike the evaporator, however, the condenser exhibits a substantial change in shell side (air) temperature, thus demanding the full form of the logarithm mean temperature difference in conditions for which the heat transfer coefficients are, in general, functions of fluid temperature. It is therefore clear that $\theta \neq \theta_c$, and h_i^c is not a constant known *ab initio*. According, the local heat balance

$$dA\dot{q}_c = dAh_i^c (T_4 - T_w^c) = dAh_o^c (T_w^c - T_a) = \dot{m}_a c_{pa} dT_a$$

has been used in satisfying the overall heat balance

$$\dot{Q}_c = \int_A \dot{q}_c^{dA}$$

This was done numerically by dividing the heat exchanger surface area into small elements, on each of which the local heat balance was used in an iterative process in which h_o^c was guessed and then refined until both local and overall heat

balances were satisfied. This extends the usual process in which the heat transfer coefficients are independent of temperature and thereby enable T_w^c to be found explicitly.

The power required to drive the condenser fan was found from the reduced form of equation (19),

$$\triangle P = 10\rho_a U^2_{max}$$

and the airflow rate, both conforming to the tube layout mentioned above. Hence

$$\dot{W}_{FAN} = 5.13\rho_a U^2_{max} \quad (25)$$

It is interesting to note that the coefficients for the pump power and fan power, which together make up the auxiliary power, are comparable; their respective densities and velocities, however, are very different.

Before leaving this section it is worth mentioning that the auxiliary fan and pump are required to withdraw just enough power from the main shaft to ensure that the heat transfer coefficients appropriate to any given speed are generated. It is thus anticipated that the offtake power would be an increasing function of engine speed. More precisely, both the fan and pump power are expected to be monotonically increasing functions of speed, concave upward, and passing through the origin. As demonstrated in Figure 7, this functionality is realized with a very strong curvature, implying that very little offtake power will be required at low speeds and that the magnitude will increase steeply in the higher speed range.

THERMAL PERFORMANCE

Given a reciprocating expander and feed pump, together with fairly conventional heat exchanger designs for the evaporator and condenser, a model of the thermal performance of the system may be developed (Lock and Stanford, 1988), with results being based on the representative environmental temperatures T_i=0°C and T_a=−25°C. The useful power is determined from equation (7), which contains both the cycle power delivered to the engine shaft and the power lost, principally to the auxiliaries. The aim is obviously to maximize the former and minimize the latter. The design speed of the engine having been deliberately taken low, it is to be expected that the internal friction loss would be especially small below the anticipated operating range. The discussion above suggests that the auxiliary power would also be small at the low end of the entire engine speed range.

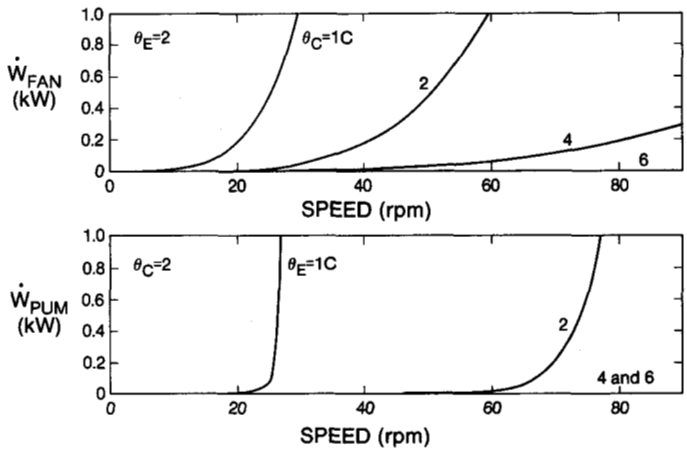

FIG. 7. Auxiliary power as a function of speed.

It is thus apparent that the useful shaft power will initially contain only the first term on the right-hand side of equation (7). As Figures 8 and 9 illustrate, the useful power increases almost linearly with engine speed until the effect of auxiliary power intervenes sharply, creating a maximum followed by a rapid decline.

Below the optimum speed, the effect of the auxiliaries is relatively small; so is the attendant dependency of the heat transfer coefficients on speed. As the optimum speed is approached and exceeded, however, speed dependency becomes an integral part of the heat exchanger calculations. For any given speed, heat transfer calculations begin with the cycle power, implicit in which are isentropic work attributable to the expander and feed pump. The difference in the isentropic works is, of course, equal to the difference between the amounts of heat transferred (per unit mass) in the evaporator and the condenser. From the consequent difference between $\dot{Q}_E$ and $\dot{Q}_C$ it is possible to determine $\dot{Q}_E$

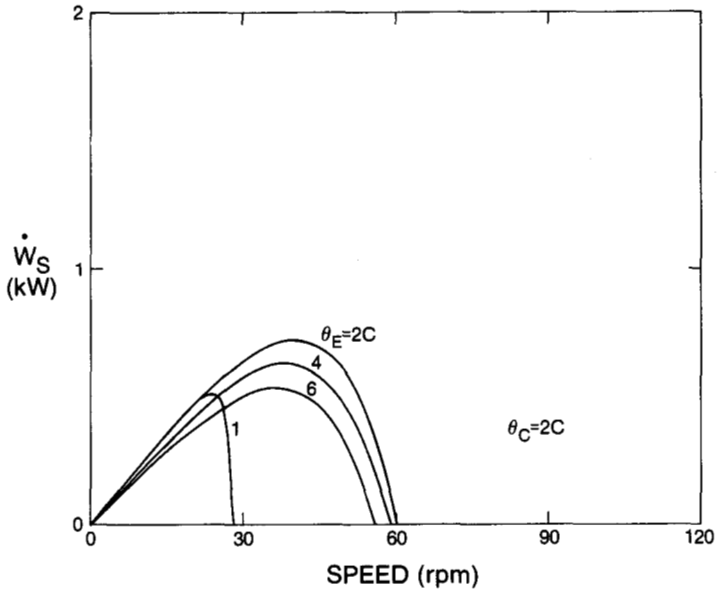

FIG. 8. Engine power as a function of speed: effect of θ_E.

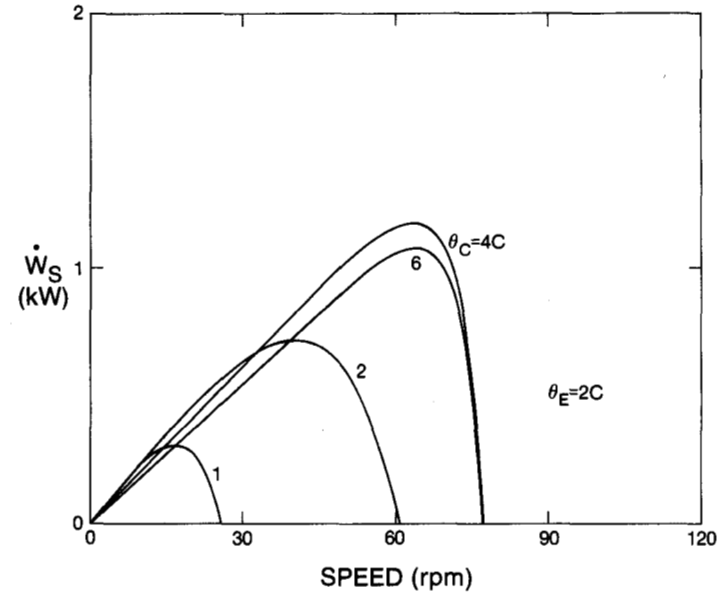

FIG. 9. Engine power as a function of speed: effect of θ_c.

and $\dot{Q}_C$ separately because of the imposed constraint that $\dot{Q}_E = \dot{m}_A \lambda_{12}$, in which the ammonia flow rate is a known function of speed.

Calculations within the evaporator begin with the desired heat transfer rate

$$\dot{Q}_E = h_i^E A_E(T_w^E - T_1) = h_o^E A_E(T_i - T_w^E) \quad (26)$$

in which the expression for h_i^E also contains the unknown wall temperature and the vapour saturation temperature T_1. It is therefore necessary to satisfy the heat balance iteratively. This was done using Newton's method, thus determining both T_W^E and h_i^E; h_o^E then follows from the equation (26), which then leads to the overall heat transfer coefficient using equation (18).

The water flow rate and velocity implicit in h_o^E fix both the pressure drop and the pump power for any particular speed, and thus complete the circle of calculations that produce corresponding pairs of $\dot{W}_c$ and $\dot{W}_{PUM}$. A similar approach may be adopted for the condenser, thus generating h_i^c and h_o^c from the heat balance, bearing in mind that neither h_i^c nor T_w^c are constants, as discussed earlier. From h_o^c follows $\dot{W}_{FAN}$. Since $\dot{W}_F$ may be found directly from the ammonia circulation rate, it is evident that each component of work may be determined at each speed, thus enabling the useful shaft power to be plotted against speed.

The shaft power-speed curves shown in Figures 8, 9 and 12 reveal that the design value of the order of 1.0 kW is attainable if the engine operates in the speed range 60-140 rpm. As anticipated, the magnitude of the power in this range is seen to be a function of θ_E and θ_c, both of which were initially, and arbitrarily, set at 2 K. For a fixed value of θ_c = 2 K, the effect of varying θ_E is to produce an optimum power level at any given speed. Since $\theta_E = T_i - T_1$, the cycle power tends to zero, while the pump power tends to infinity as $\theta_E \to 0$. The optimum value of θ_E for this engine configuration varies with speed but is about 1.7.

From Figure 9 it is evident that the same sort of result is produced if θ_E = 2 K and θ_c is varied, the optimum being near θ_c = 3 K. No attempt was made to find the corresponding pairs of optima for each speed, but the extent of the possible power gain was explored using rough estimates in the operating speed range, specifically in the vicinity of 80 rpm. Figure 12 shows that with θ_c = 5 K and θ_E = 3 K, the maximum power attainable is increased 100% over that for the nominal values of $\theta_E = \theta_c$ = 2 K.

An important feature of the power-speed curve is its changing slope over the speed range considered. In fact, the operating range is essentially delineated by the requirement that the curve slope be negative in order to enhance, if not ensure, load stability. In this range, the greater the speed the steeper the curve but the lower the power, thus requiring a compromise that balances the output of the engine against the tolerance of speed fluctuations. The precise point of balance would obviously be determined from the demands of the particular application.

The efficiency of the engine is explored in Figures 10 and 11. As expected, the overall efficiency is higher at lower speeds when losses are very small. Overall efficiencies in excess of 6% are then attainable. With increasing speed and sharply increasing losses, the efficiency drops off dramatically, reaching zero at the point where the shaft power is also zero. Typical magnitudes in the appropriate operating speed range are in excess of 4% when $\theta_c = \theta_E$ = 2 K.

To examine engine performance in relation to the Carnot cycle, the efficiency ratio and shaft power have been plotted against speed for two pairs of θ's in Figure 12. In the appropriate operating range, the efficiency of the engine exhibits a maximum with respect to both θ_c and θ_E, the reasoning being precisely that given for the corresponding power maximum, as equation (9) would require. The effect of optimization on overall efficiency is immediately evident from this equation: the effect is seen in Figures 10 and 11. Doubling the power level while doubling the speed produces no change in the specific shaft work and would leave the overall efficiency unchanged.

The highest value of efficiency ratio occurs at zero speed. Near this point, where heat exchanger characteristics are no longer important, neither the power nor the efficiency exhibits

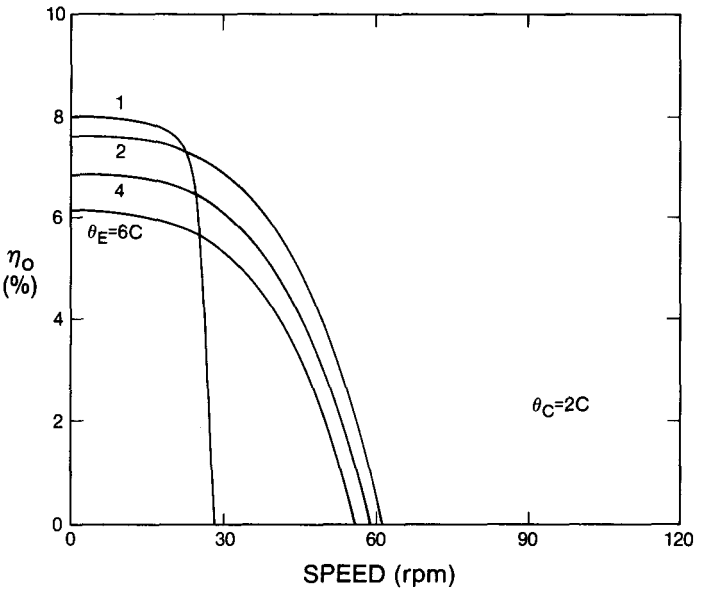

FIG. 10. Overall efficiency as a function of speed: effect of θ_E.

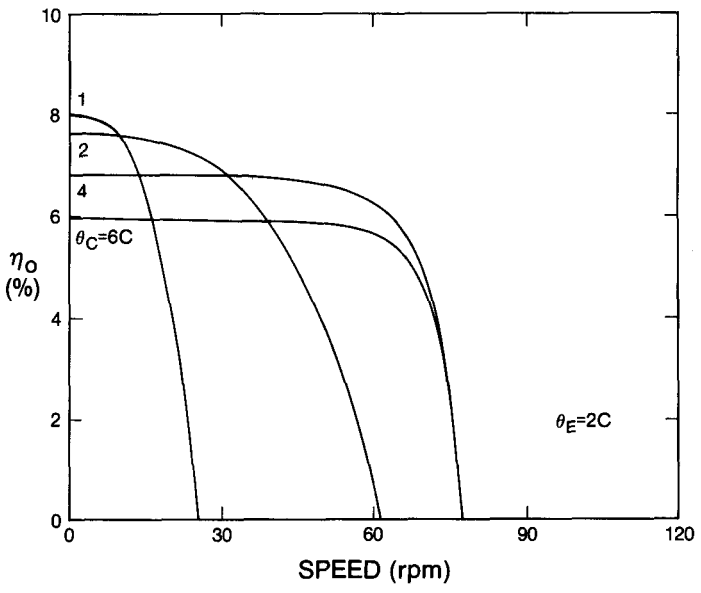

FIG. 11. Overall efficiency as a function of speed: effect of θ_c.

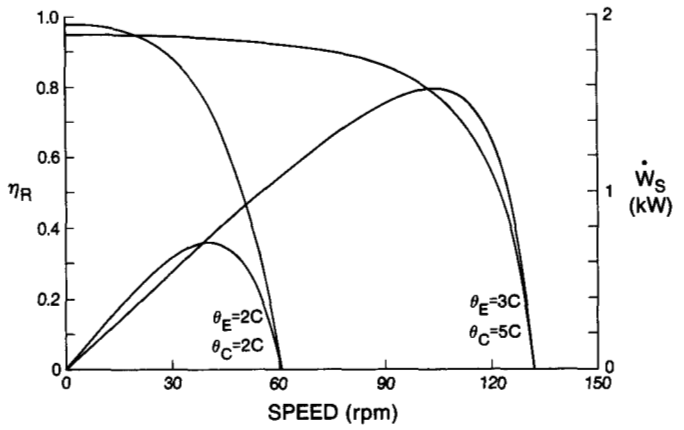

FIG. 12. Power and efficiency as functions of speed.

an optimum with respect to either of the θ's. Instead, the effect of decreasing θ is to monotonically increase both the shaft work and the efficiency, as illustrated in Figures 9-11. Figure 11, in particular, reveals a very close approach to the Carnot efficiency at these speeds. In the operating speed range, the efficiency ratio has dropped below 40%, but even this value is encouragingly high, especially in the context of a marginal energy source.

GENERAL CONSIDERATIONS

The cylinders of the reciprocating expander and feed pump may be oriented in any direction. Evenness of wear is better accommodated in the vertical position, but ease of maintenance, which is perhaps an overriding concern, would suggest the horizontal position. Both expander and feed pump are envisaged as single-cylinder, double-acting devices, thus smoothening the shaft power delivery and improving the power density, although none of these features is affected by cylinder orientation. The two cylinders may be in line (side by side), at 90 degrees, or opposite each other, so long as their relative phase displacement on the crank is appropriately chosen. Smoother operation is likely to result from phase opposition, but this need not dictate cylinder orientation. However, physical separation lends itself both to ease of maintenance and to the placing and connecting of the heat exchangers. Hence the horizontally opposed arrangement appears to offer most advantages.

In this configuration, the forces acting on the expander piston are, generally speaking, opposed by those acting on the feed pump piston. With respect to the expander alone, the net piston force is essentially the variable expansive force minus the more or less constant back pressure corresponding to exhaust on the other side of the piston; only during the late stages of the return stroke, when the exhaust valve has closed, does the balance change significantly. From this net driving force must be subtracted the net force on the feed pump piston. Although the pressure limits are the same for expander and feed pump, the latter has a much smaller area and acts only during the discharge period.

Both of the net piston force relationships may be converted into a torque-crank angle diagram from which it is estimated that torque variations would be fairly large. This is not surprising for a single-cylinder machine, even though it is double acting. In this configuration a large coefficient of fluctuation may result. There are many field applications, such as the pumping of fluids, where speed fluctuations are not important, but there are others, such as electrical power generation, where the fluctuations must be matched to the specific application using any of a variety of strategies: suitable flywheels, gearing, inertial characteristics of auxiliaries and driven device, multi-cylinder arrangements, etc.

Another important dynamic characteristic of the engine is the control of speed. The cycle power is clearly a linear, increasing function of speed that is inherently unstable. The frictional power required to circulate the working fluid does not alter this significantly because the frictional loss is so low: the slope of the shaft power-speed curve would remain positive if internal friction was accommodated over the speed range considered. On the other hand, the offtake power required to drive the fan and water pump increases much more rapidly with speed than does the cycle power. As demonstrated earlier, the net shaft power eventually reaches a maximum and then begins to fall. This descending section of the curve is inherently stable: a decreased load accelerates the shaft but only until the additional cycle power is balanced by an increase in the more rapidly rising offtake power; the reverse is true for an increased load.

In a more conventional situation, speed control may be effected with an automatic feedback throttling device such as a Watt governor and valve combination. Choosing to operate the present expander at speeds beneath the power maximum would also demand the use of a throttling device. At first sight, this may appear to be a serious disadvantage with a marginal energy source, but closer examination suggests otherwise. Using the data in Table 1, for example, it is evident that the pressure drop across the expander is 278 kPa when ammonia is used between the given temperature limits. Without attempting to prescribe the precise pressure drop versus speed characteristics of the throttling valve, it is evident that only a few percent of this overall drop is needed for effective control. However, a better design choice would be operation just above the power maximum. This could reduce the role of the throttling value to one of fine tuning and may eliminate it entirely.

Given that the principal aim of this study is to develop a model of a modular hydrothermal engine designed to operate reliably and unattended in remote northern regions, it is logical that the level of technology should be kept to a minimum. The use of well-established reciprocating vapour engine theory and practice satisfied this objective in the machinery design. The use of conventional heat exchanger theory, although complicated by the introduction of transients and temperature-dependent heat transfer coefficients, enabled the model to be completed in the form described by equation (7), from which the optimum shaft power is given by

$$(\dot{W}_s)_{opt} = \tau N_{opt} - f(N_{opt})$$

in which the optimum speed is determined at $d\dot{W}_s/dN = O$; that is, $f'(N_{opt}) = \tau$, where the prime denotes differentiation with respect to N. The inherently stable range of the operating curve is therefore defined by

$$N_{opt} \leq N \leq N_{max}$$

where $\tau N_{max} = f(N_{max})$ marks the upper limit of engine speed. Any particular design of the expander and feed pump operating between prescribed saturation pressures (or tem-

peratures) essentially fixes the engine cycle torque τ. The function f(N) is determined from the characteristics of the heat exchangers: it will be a monotonic, and steeply rising, function such that f(o) = O.

The heat exchanger configurations specified were sufficient to illustrate the basic behaviour of the engine but need to be examined much more closely if the modular design is to find widespread use. Pulsatility, for example, has merely been considered as a quasi-steady phenomenon. Although this may be a permissible approximation, it needs to be supported by transient boiling and condensation data, which are currently unavailable. More important, the ranges of θ_E and θ_c attainable in practice need further discussion.

The nominal choice of $\theta_E = \theta_c = 2$ K reveals that the rated shaft power is attainable, but Figure 7 emphasizes how sensitive the auxiliary power is to the temperature loss. It is clear that $\theta < 1$ K implies fan and pump powers great enough to bring the engine to a halt. On the condenser side, the problem may be removed by allowing $\theta_c > 4$ K, as Figures 9, 11 and 12 suggest. For this condition, h_o^c was typically less than 100 $W \cdot m^{-2}K^{-1}$ at 60 rpm (Lock and Stanford, 1988), thus raising the practical possibility of wind augmentation. Average wind speeds in excess of 5 $m \cdot s^{-1}$ are common in northern Canada (Fletcher and Young, 1976).

At first sight, Figure 7 suggests that the pump power could be maintained within reasonable bounds if $\theta_E \geq 2$ K, at least up to 70 rpm. However, this apparently modest objective is very difficult to attain in northern lakes, rivers and oceans when they are covered in ice. There is no single remedy, but there are two strategies that are generally applicable, separately or in combination: to transfer sensible heat to the water from another source that is not too distant; and to use the latent heat capacity of water. Depending upon the site, a nearby heat source may be found in a power plant discharge, a geothermal fissure, an ocean current or a stratified lake; river water is usually very close to the freezing point and may be supercooled (Ashton, 1986). With the exception of geothermal sources, which are obviously limited in distribution, the temperature of a natural source is likely to be only 1 or 2 K above the freezing point of the water. The proximity of the source will therefore dictate the pumping and thermal insulation requirements necessary to transfer the sensible heat to the site of the engine. Although it is impossible to generalize, the most likely prospect for success would appear to be when the source lies directly beneath the site, for this permits the use of natural buoyancy forces to effect the transfer with minimum, and perhaps zero, pumping requirements. In a stable stratified lake, for example, the sensible heat could be transferred vertically using heat pipes, thermosyphons or aerosyphons. From studies of aerosyphons (Lock and Maezawa, 1975; Lock and Kirchner, 1987) it is estimated that a 1.0 m diameter pipe can transfer 1.5 kW over a vertical distance of about 100 m when the upper temperature is only 1 K beneath the temperature at depth. Although no heat transfer data are currently available for full-scale tests on systems of this type, it is reasonable to expect that some, and perhaps all, of the sensible heat necessary to maintain $\theta_E \geq 1$ K could be supplied in this manner. Direct bubbling is another possibility, but it permits mixing of the aerated plume and may be uneconomical in its power demands, depending on the bottom water temperature and the extent of the lift.

The second strategy comes into play when θ_E is small enough to permit freezing of the water circulating through the evaporator. If so, an additional thermal resistance t_i/k_i, where t_i is the ice thickness, must appear in equation (18). In essence, this is simply a modification of F_o. With $t_i/k_i = 0(10^{-3})$, for 2.0 mm thick ice, the additional "fouling" factor is comparable with the external convective resistance (Lock and Stanford, 1988). The overall temperature loss θ_E is then divided roughly equally between the water and the ice, with a much smaller drop occurring in the ammonia. Thus when $\theta_E = 2$ K, about 1 K occurs in the water.

The presence of ice is not necessarily detrimental unless it begins to block the water flow and thereby increases the pumping power and/or decreases the heat exchange rate, in which case sensible heat transfer may have to be abandoned in favour of latent heat transfer. The role of the ice could be replaced with a liquid anti-freeze acting as a secondary coolant between the water and the evaporator tubes, but only at the expense of additional pumping power. Under such circumstances it may be better to use the storage capacity inherent in the freezing process. This may be accomplished in two ways: allowing direct contact between the water and the working fluid to generate ice crystals; and allowing the water on the outside of the evaporator tubes to freeze completely.

The first of these two methods uses the concept of a crystallizer boiler in which the working fluid is dispersed in droplet form throughout the water supply (Haydock, 1985). The latter, having a slightly greater temperature, supplies thermal energy, partly as sensible heat but mostly as latent heat. The dispersed droplets ensure a large surface area for heat transfer between the two substances, both initially liquids. Under suitable conditions, the working fluid is vapourized at its saturation pressure while the water is partially converted to ice through the process of nucleation and crystal growth. The saturated vapour is then directed into the expander and the ice-water slush is returned to the body of water from which it was drawn. This approach has the merit of being able to employ a very small temperature loss θ_E but the demerit of requiring pumping power.

The second method simply replaces heat transfer by convection in water with conduction through ice. To obtain a comparable heat transfer rate, the thermal resistance of the ice would have to be the inverse of the water heat transfer coefficient. As implied earlier, $h_o^E = 0(10^3)$ typically, so that the corresponding ice thickness must be of the order of 2.0 mm. A greater thickness would demand a compensatory increase in the surface area of the evaporator tubes. In the design discussed earlier, evaporator and condenser tubes were given the same diameter, their surface areas therefore being in direct proportion to the total length of tubing. Since the length of tubing incorporated into the evaporator was only 10% of that needed for the condenser, the scope for increased evaporator tube area is evidently great. If the evaporator surface area was made equal to the condenser surface area, for example, h_o^E could be reduced to $0(10^2)$. Each evaporator tube could then be embedded in a cylinder of ice as large as 6.0 cm in diameter; with the temperature difference across the ice ($\simeq \theta_E$) being only 1 K, the instantaneous heat transfer rate would still be 15 kW. The volume of ice thus produced represents a latent heat transfer rate of 15 kW for about 1.5 days. Further increases in ice thickness would compromise

the heat transfer rate unless θ_E was allowed to increase, but this would only provide limited flexibility. A more logical course of action would be to remove the ice and begin the freezing process anew. De-icing may be readily accomplished by raising the saturation temperature of the ammonia in the evaporator above T_i just long enough to melt the ice molecules immediately adjacent to the outer surface of the tubes. Careful design would ensure that the ice could then float free of the evaporator. A potential demerit of this approach is the need to increase the total length of evaporator tubing; the obvious merit is the complete elimination of pumping power.

Finally, a few comments on temperature control. In a typical situation the water (or ice) temperature is not likely to change very much during the operating period when an ice cover caps the heat source. However, the air temperature may vary considerably. Assuming the design value of T_a has been chosen conservatively, the actual air temperature is more likely to lie below the design value than above it. Excursions below the design value potentially lead to greater heat transfer rates by increasing θ_c. Since this would produce a subcooled liquid, with no thermodynamic benefit, it would best be avoided, either through compensatory reductions in fan power or, perhaps more conveniently, by partial closing of a louvered air inlet. Small excursions of T_a above the design value, i.e., $T_a \lesssim T_4$, would cause a reduced heat transfer rate and thus cause a reduction in shaft power; opening of a louvered inlet may provide a partial remedy. Should T_a exceed T_4, the engine would shut down.

CONCLUSIONS

A model of a reciprocating Carnot cycle engine has been developed for conditions representative of a polar or subpolar winter. With a hydrothermal heat source at 0°C and an atmospheric heat sink at −25°C, the model has been used to examine the characteristics and requirements of a 1.0 kW engine using fairly conventional theory and practice for the design of the evaporator and condenser. The power output of the engine was found to rise steadily with speed before exhibiting a maximum followed by a very sharp decline. This behaviour reflects the monotonically, and sharply, increasing power demands of the auxiliaries. The engine is inherently stable with respect to load for speeds in excess of the optimum value. It was shown that the engine efficiency reached levels at least as high as those suggested for comparable OTEC systems.

The principal difficulty with hydrothermal engines operating in polar or subpolar regions arises from the small temperature differences (losses) occurring in the heat exchangers. In the condenser, this loss does not constitute a major technical problem, but it may be viewed as an economic problem because of the capital cost incurred in building a large air-cooled heat exchanger. Against this potential limitation must be set three important facts: wind augmentation may be used to reduce fan power; annual operating (fuel) costs of conventional power generators in current use are comparable with their capital costs; and the unit capital cost of small power modules may be reduced substantially through mass production.

Small temperature differences across the evaporator do create a technical problem which, although formidable, is by no means insuperable. To combat this difficulty, two strategies have been advanced. The first suggests alleviation of the difficulty by tapping a neighbouring heat source lying beneath the site, specifically through the use of thermosyphons or aerosyphons. The second suggests the use of latent heat exchangers that either build ice around the evaporator tubes *in situ* or create it in dispersed crystals that are discharged back into the main body of water. In combination, these strategies could free the engine from its location on a large body of water. Given the design specifications considered in this paper, for example, the volume of ice created by an *in situ* heat exchanger, about 500 m^3 (15×10^{10} J) over a three-month period, could be contained in a buried tank below the floor of which thermosyphons might be installed. Such an arrangement would permit either the convective or the latent heat transfer mode of operation; it would also make possible either higher shaft powers or an extended season, and perhaps both.

Potential applications of this type of engine are numerous and cover practical power levels ranging from 1 to 100 kW at least. The smaller end of this spectrum would be appropriate for a remote and automatic scientific station or for a small group of people with the usual daily requirements in heating, lighting, cooking, communications, etc. The larger end would be more appropriate to a small settlement or industrial plant. The modular concept lends itself to covering the entire spectrum. For example, if modules were produced with rated power levels of 2, 10 and 50 kW, it would be possible to match virtually any likely power need through the simple measure of ganging. Furthermore, the use of modules increases the flexibility of capital by accommodating the growth (or reduction) of power demand in small increments that are easily satisfied; and, as noted earlier, the manufacture of a large number of small modules greatly reduces the unit capital cost.

ACKNOWLEDGEMENTS

This work was undertaken with the support of the Department of Energy, Mines and Resources, to whom I am grateful.

REFERENCES

ASHRAE. 1985. Handbook of Fundamentals. Atlanta: American Society of Heating, Refrigeration and Air-conditioning Engineers.

ASHTON, G.D., ed. 1986. River and Lake Ice Engineering. Littleton: Water Resource Publications.

CARNOT, S. 1960. Reflections on the motive power of fire, and on machines fitted to develop that power. In: Mendoza, E., ed. Reflections on the Motive Power of Fire and Other Papers. New York: Dover Publications Inc. 3-22.

CHATO, J.C. 1962. Laminar condensation inside horizontal and inclined tubes. Journal American Society of Heating, Refrigeration and Air-conditioning Engineers 4:52-61.

CHEN, J. 1966. Correlation for boiling heat transfer to saturated liquids in convection flow. Industrial Engineering Chemistry, Processes, Design and Development 5:322-328.

EL-WAKIL, M.M. 1984. Powerplant Technology. New York: McGraw Hill Book Co. 628-631.

FLETCHER, R.J., and YOUNG, G.S. 1976. Climate of Arctic Canada in Maps. Edmonton: Boreal Institute for Northern Studies, Occasional Publications 13.

GOSNEY, W.B. 1982. Principles of Refrigeration. Cambridge: Cambridge University Press. 122.

HAYDOCK, J.L. 1985. Electrical energy production from water/air temperature differences in the arctic. Report prepared for Canadian Electrical Association by Acres International Ltd.

LOCK, G.S.H., and KIRCHNER, J.D. 1987. Performance of a closed tube aerosyphon with large length-diameter ratios. Proceedings of the International Symposium on Cold Regions Heat Transfer. American Society of Mechanical Engineers. 261-270.

LOCK, G.S.H., and MAEZAWA, S. 1975. The aerosyphon: an exploratory study. International Journal of Heat and Mass Transfer 8:219-226.

LOCK, G.S.H., and STANFORD, H.K. 1988. Performance analysis of a reciprocating polar Carnot cycle engine. Proceedings of the 7th International Conference on Offshore Mechanics and Arctic Engineering. American Society of Mechanical Engineers.

McNAUGHTON, E. 1948. Elementary Steam Power Plant Engineering. New York: J. Wiley and Sons. 417.

MOCHIDA, Y., KAWANO, S., TAKAHATA, T., and MIYOSHI, M. 1984. Performance of the heat exchangers of a 100kW (Gross) OTEC Plant. Journal of Solar Energy Engineering 106:187-192.

ROGERS, G.F.C., and MAYHEW, Y.R. 1967. Engineering Thermodynamics, Work and Heat Transfer. 2nd ed. London: Longmans. 398.

RZANJEVIC, K. 1976. Handbook of Thermodynamic Tables and Charts. New York: Hemisphere Publishing Co.

SWARTMAN, R.K., and GREEN, R. 1978. An ocean thermal difference power plant in the Canadian arctic. Proceedings of the 4th Conference on Renewable Energy Alternatives, University of Western Ontario.

TAYLOR, R.H. 1983. Alternative Energy Sources. Bristol: Adam Hilger Ltd. 120-150.

TEMA. 1959. Standards. New York: Tubular Exchanger Manufacturers Association.

UEHARA, H., KUSUDA, H., MONDE, M., and NAKAOKA, T. 1984. Shell-and-plate type heat exchangers for OTEC plants. Journal of Solar Energy Engineering 106:286-290.

WARRING, R.H. 1984. Pumps: Selections, Systems and Applications. Houston: Gulf Publishing Co. 5-6.

ZUKAUSKAS, A. 1972. Heat transfer from tubes in cross flow. New York: Academic Press. Advances in Heat Transfer 8:93-160.